Aerodynamic and Structural Detuning of Supersonic Turbomachine Rotors

Daniel Hoyniak*
NASA Lewis Research Center, Cleveland, Ohio
and
Sanford Fleeter†
Purdue University, West Lafayette, Indiana

A mathematical model is developed to predict the unstalled torsion mode flutter of an aerodynamically and structurally detuned rotor operating in a supersonic inlet flowfield with a subsonic leading-edge locus. Alternate blade structural detuning is considered. The aerodynamic detuning is accomplished by alternating the circumferential spacing of adjacent rotor blades. The unsteady aerodynamics are defined in terms of influence coefficients. To demonstrate the effects of aerodynamic and structural detuning on supersonic unstalled torsional flutter, a 12 bladed rotor based on Verdon's cascade B flow geometry is considered. Aerodynamic and structural detuning are individually shown to enhance the stability of the baseline rotor, although neither technique stabilizes the rotor over the complete reduced frequency range considered. The greatest stability enhancement, with the resulting rotor stable over the complete reduced frequency range, results from combined aerodynamic and structural detuning.

Nomenclature

c	= airfoil chord
C	= perturbation sonic velocity
C_M^n	= influence coefficient of airfoil n
ΔC_p	= $\Delta p/\frac{1}{2}\rho u_\infty^2$
$C_{\alpha\alpha}$	= unsteady aerodynamic moment
I	= mass moment of inertia per unit span
k	= reduced frequency, $k=\omega c/u_\infty$
M	= dimensionless unsteady aerodynamic moment
M_∞	= cascade inlet Mach number
P	= perturbation pressure
ΔP	= perturbation pressure difference
S	= airfoil spacing
u_∞	= cascade inlet velocity
U	= perturbation chordwise velocity
V	= perturbation normal velocity
x	= dimensional chordwise coordinate
y	= dimensional chordwise corrdinate
α	= amplitude of oscillation
$\hat{\alpha}$	= complex oscillatory amplitude
β	= interblade phase angle
ϵ	= level of aerodynamic detuning
ρ	= air density
ω	= oscillatory frequency
[ ]	= matrix

Subscripts

d	= detuned cascade
n	= airfoil number
R	= reference airfoil of uniformly spaced cascade
R_e, R_o	= reference for set of even or odd numbered airfoils of detuned cascade

Presented as Paper 85-0761 at the AIAA/ASME/ASCE/AHS 25th Structures, Structural Dynamics and Materials Conference, Orlando, FL, April 15-17, 1985; received April 25, 1985; revision received Sept. 24, 1985. This paper is declared a work of the U.S. Government and therefore is in the public domain.

*Aerospace Engineer.
†Professor, School of Mechanical Engineering and Director, Thermal Sciences and Propulsion Center.

Introduction

THE aeroelastic stability analysis of gas turbine engine bladed disk assemblies is simplified by assuming that the blades are identical, having uniform mass and stiffness properties, i.e. a tuned rotor configuration. However, the blades of a single rotor have a range of natural frequencies due to manufacturing tolerances. These random airfoil-to-airfoil variations in natural frequency are defined as structural mistuning, the first discussion of which was presented by Whitehead.[1]

Recent reviews of existing flutter data indicate that the stability characteristics of a rotor can be affected by this random structural mistuning. This interesting result has led to the investigation of structural detuning, defined as designed airfoil-to-airfoil variations in blade natural frequencies, as a passive control mechanism to eliminate flutter from the operating range of an engine. Several studies have indicated that structural detuning can provide a substantial improvement in aeroelastic stability.[2-6]

A new approach to passive flutter control is aerodynamic detuning, defined as designed passage-to-passage variations in the aerodynamic flowfield of a rotor blade row. Thus, aerodynamic detuning results in blade-to-blade differences in the unsteady aerodynamic forces and moments acting on a blade row. This results in the blading not responding in a classical traveling wave mode typical of the flutter behavior of a conventional aerodynamically tuned rotor. Thus, aerodynamic detuning directly affects the fundamental driving mechanism for flutter, the unsteady aerodynamic forces and moments acting on individual rotor blades.

In this paper, the enhanced flutter stability of a turbomachine rotor associated with combinations of aerodynamic and structural detuning is analyzed. In particular, a mathematical model is developed to predict the aeroelastic stability of an aerodynamically and structurally detuned rotor operating in a supersonic inlet flowfield with a subsonic leading-edge locus. Alternate blade structural detuning is considered, a technique that has been shown to be optimal when errors in implementation are considered.[5] The aerodynamic detuning is accomplished by means of nonuniform circumferential spacing of adjacent rotor blades.

Unsteady Aerodynamic Model

For supersonic unstalled flutter, a flat-plate airfoil cascade embedded in a supersonic inlet flowfield with a subsonic leading-edge locus undergoing torsion mode harmonic oscillations is considered. See Fig. 1. The fluid is assumed to be an inviscid, perfect gas with the flow isentropic, adiabatic, irrotational, and two-dimensional. The unsteady continuity and Euler equations are linearized by assuming that the unsteady perturbations are small as compared to the uniform throughflow. Thus, the boundary conditions, which require the unsteady flow to be tangent to the airfoil surfaces and normal velocity to be continuous across the wake, are applied on the mean positions of the oscillating airfoils.

The unsteady cascade aerodynamics and, in particular, the unsteady forces and moments acting on the uniformly spaced airfoils are predicted using various techniques. Of particular interest are the analyses of Verdon and McCune,[6] Brix and Platzer,[7] and Caruthers and Riffel.[8] These analyses utilize a finite cascade representation of the semi-infinite cascade. The cascade periodicity condition is enforced by stacking sufficient numbers of uniformly spaced single airfoils until convergence in the unsteady flowfield is achieved.

For the aerodynamically detuned, alternate nonuniform circumferentially spaced rotor, an analogous unsteady aerodynamic model is utilized. In particular, the unsteady aerodynamics associated with the small-perturbation torsion mode harmonic oscillations of a nonuniformly spaced, two-dimensional, flat-plate airfoil cascade embedded in an inviscid, supersonic inlet flowfield with a subsonic leading-edge locus is considered.

The analysis of this type of configuration is most easily accomplished utilizing a finite cascade representation of the semi-infinite cascade (Fig. 2). As seen, there are two distinct flow passages: a reduced spacing or increased solidity passage, and an increased spacing or reduced solidity passage. Also, the detuned cascade is composed of two separate sets of airfoils. For convenience, these are termed the set of odd-numbered airfoils and the set of even-numbered airfoils. Thus, two passage periodicity is required for this detuned cascade, i.e., the periodic cascade unsteady flowfield is achieved by stacking sufficient numbers of two nonuniform flow passages or two airfoils, one from each set.

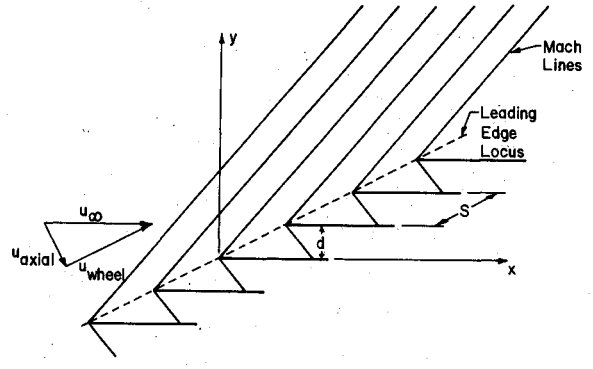

Fig. 1 Flat-plate airfoil cascade in a supersonic with subsonic axial component inlet flowfield.

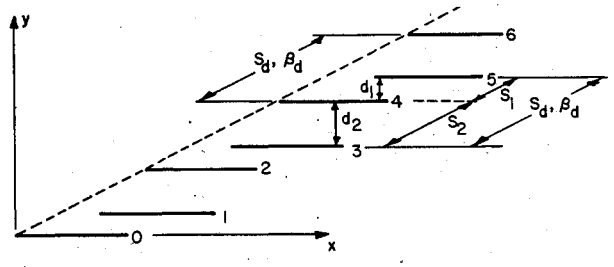

Fig. 2 Finite cascade representation for alternate nonuniform circumferential spacing aerodynamic detuning.

The formulation of the linearized differential equations describing the unsteady perturbation quantities for the finite aerodynamically detuned cascade is based on the method-of-characteristics analysis of the finite uniformly spaced airfoil cascade developed by Brix and Platzer.[7] In particular, the dependent variables are the nondimensional chordwise, normal, and sonic perturbation velocities, U, V, and C, respectively. The independent variables are the chordwise and normal coordinates normalized by the airfoil chord, x and y, and time t. Assuming harmonic motion at a frequency ω, the resulting set of differential equations describing the unsteady perturbation flowfield are

$$\frac{\partial U}{\partial x}+\sqrt{M_\infty^2-1}\,\frac{\partial V}{\partial y}+\frac{\partial C}{\partial x}+ikM_\infty^2 C=0$$

$$\frac{\partial U}{\partial x}+\frac{\partial C}{\partial y}+ikU=0$$

$$\frac{\partial U}{\partial y}-\sqrt{M_\infty^2-1}\,\frac{\partial V}{\partial x}=0 \qquad (1)$$

The flow tangency boundary condition requires that the normal perturbation velocity component V be equal to the normal velocity of the airfoil surfaces on the mean position of the oscillating airfoils. For an airfoil cascade executing harmonic torsional motions about an elastic axis located at x_0 as measured from the leading edge, the dimensionless normal perturbation velocity component on the nth airfoil is specified as

$$V_n(x,y_s,t)=-\alpha_n[1+(x-x_0)ik]e^{i(kt+n\beta)} \qquad (2)$$

where $y_s=y_s(x)$ denotes the airfoil surface.

Solutions for the unknown chordwise, normal, and sonic dimensionless perturbation velocities U, V, and C in each of the two periodic flow passages of the semi-infinite cascade are then determined by means of the two airfoil passage stacking technique in conjunction with a finite difference method of characteristics scheme. The periodic perturbation unsteady surface pressure distributions are determined from these perturbation velocities by means of the linearized unsteady Bernoulli equation. The nondimensional unsteady aerodynamic moment acting on the reference airfoils, M_R, are then calculated by integrating the unsteady surface perturbation pressure difference across the chordline.

$$M_R=\int_0^1 \Delta P(x,y_s,t)\,(x-x_0)\mathrm{d}x \qquad (3)$$

Aerodynamic Influence Coefficients

The aerodynamically detuned nonuniformly spaced cascade is composed of two distinct flow passages and sets of airfoils, termed odd and even numbered. Thus, two reference airfoils, R_o and R_e, are required. The unsteady aerodynamic moments acting on these two reference airfoils are defined in terms of the following influence coefficients.

$$\begin{aligned}M_{R_o,R_e}&=\{\hat\alpha_1[C_M^1]_{R_o,R_e}+\hat\alpha_3[C_M^3]_{R_o,R_e}+\dots\\&+\hat\alpha_{R_o}[C_M^{R_o}]_{R_o,R_e}+\dots+\hat\alpha_N[C_M^N]_{R_o,R_e}\}e^{i\omega t}\\&+\{\hat\alpha_0[C_M^0]_{R_o,R_e}+\hat\alpha_2[C_M^2]_{R_o,R_e}+\dots\\&+\hat\alpha_{R_e}[C_M^{R_e}]_{R_o,R_e}+\dots+\hat\alpha_{N-1}[C_M^{N-1}]_{R_o,R_e}\}e^{i\omega t}\end{aligned} \qquad (4)$$

where, $[C_M^n]_{R_o,R_e}$ denotes the influence coefficient on the reference airfoil R_o or R_e associated with the motion of airfoil number n. Physically, it represents the unsteady aerodynamic

moment acting on the fixed reference airfoil, R_o or R_e, due to unit amplitude motion of airfoil number n.

The two groups of bracketed terms in Eq. (3) are associated with the motion of the sets of odd and even-numbered airfoils, respectively. The complex amplitude of harmonic oscillation for the set of odd-numbered airfoils is denoted by $\hat{\alpha}_{R_o} \exp i[\omega t + n\beta_d]$, where β_d defines the constant interblade phase angle between the sequentially odd-numbered airfoils. Similarly, the set of even-numbered airfoils are assumed to oscillate with the complex amplitude $\hat{\alpha}_{R_e} \exp i[\omega t - n\beta_d]$, where β_d is the same interblade phase angle as utilized for the odd-numbered airfoils. The phase difference between the motions of the sets of odd- and even-numbered airfoils is accounted for in that $\hat{\alpha}_{R_o}$ and $\hat{\alpha}_{R_e}$ denote complex amplitudes. Thus, the unsteady moments acting on the two reference airfoils can be written in matrix form as

$$\begin{bmatrix} M_{R_o} \\ M_{R_e} \end{bmatrix} = \begin{bmatrix} [CM^1]_{R_o} & [CM^2]_{R_o} \\ [CM^1]_{R_e} & [CM^2]_{R_e} \end{bmatrix} \begin{bmatrix} \hat{\alpha}_{R_o} \\ \hat{\omega}_{R_e} \end{bmatrix} e^{i\omega t} \tag{5}$$

where

$$[CM^1]_{R_o,R_e} = [C_M^{R_o}]_{R_o,R_e} + e^{i\beta_d}[C_M^3]_{R_o,R_e} + \ldots$$

$$+ e^{i[(N-1)/2]\beta_d}[C_M^N]_{R_o,R_e}$$

$$[CM^2]_{R_e,R_o} = [C_M^{R_e}]_{R_o,R_e} + e^{i\beta_d}[C_M^2]_{R_o,R_e} + \ldots$$

$$+ e^{i[(N-3)/2]\beta_d}[C_M^{N-2}]_{R_o,R_e}$$

The terms $[CM^1]_{R_o,R_e}$ describe the influence that the set of odd-numbered airfoils has on the unsteady moment developed on reference airfoils R_o and R_e, respectively. $[CM^2]_{R_o,R_e}$ represent the effect that the set of even numbered airfoils has on these two reference airfoils. The expressions given above for $[CM^2]_{R_o,R_e}$ and $[CM^1]_{R_o,R_e}$ were developed assuming that $R_e = 0$ and $R_o = 1$; other choices of the reference airfoil could have been made, but the resulting expressions would have taken a more complicated form.

Equations of Motion

The equations describing the single degree-of-freedom torsional motion of the two reference airfoils of the nonuniformly spaced cascade are developed by considering the typical airfoil sections depicted in Fig. 3. Positive torsional displacements are defined as a clockwise motion such that the blade is in a leading-edge-up configuration. The elastic restoring forces are modeled by linear torsional springs at the elastic axis location, with the inertial properties of the airfoils represented by their mass moment of inertia about the elastic axis. The following equations of motion are then determined using Langrange's technique.

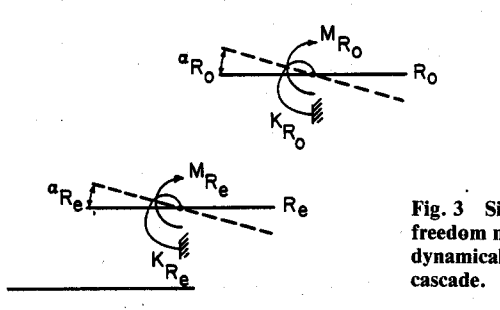

Fig. 3 Single degree-of-freedom model for aerodynamically detuned cascade.

$$I_{\alpha_{R_e}}\ddot{\alpha}_{R_e} + (1 + 2ig_{\alpha_{R_e}})I_{\alpha_{R_e}}\omega_{\alpha_{R_e}}^2\alpha_{R_e} = M_{R_e}$$

$$I_{\alpha_{R_o}}\ddot{\alpha}_{R_o} + (1 + 2ig_{\alpha_{R_o}})I_{\alpha_{R_o}}\omega_{\alpha_{R_o}}^2\alpha_{R_o} = M_{R_o} \tag{6}$$

where the undamped natural frequencies are

$$\omega_{\alpha_{R_e}}^2 = K_{\alpha_{R_e}}/I_{\alpha_{R_e}}; \qquad \omega_{\alpha_{R_o}}^2 = K_{\alpha_{R_o}}/I_{\alpha_{R_o}}$$

and $g_{\alpha_{R_e}}$ and $g_{\alpha_{R_o}}$ denote the structural damping coefficients for reference airfoils R_e R_o, respectively.

Considering harmonic motion of the reference airfoils and utilizing the unsteady aerodynamic moments defined in Eq. (5), the single degree-of-freedom torsion mode equations of motion can be expressed in nondimensional matrix form as

$$\begin{bmatrix} \mu_e & [CM^1]_{R_e} \\ [CM^2]_{R_o} & \mu_0 \end{bmatrix} \begin{bmatrix} \hat{\alpha}_{R_e} \\ \hat{\alpha}_{R_o} \end{bmatrix} = \begin{bmatrix} 0 \\ 0 \end{bmatrix} \tag{7}$$

where

$$\mu_e = \mu_{R_e} r_{\alpha R_e}^2 + [CM^2]_{R_e} - [1 + 2ig_{\alpha R_e}]\mu_{R_e} r_{\alpha R_e}^2 \gamma_{\alpha R_e}^2 \gamma$$

$$\mu_o = \mu_{R_o} r_{\alpha R_o}^2 + [CM^1]_{R_o} - [1 + 2ig_{\alpha R_o}]\mu_{R_o} r_{\alpha R_o}^2 \gamma_{\alpha R_o}^2 \gamma$$

$$\mu_{R_e,R_o} = \frac{m_{R_e,R_o}}{\pi \rho b^2}; \qquad r_{\alpha R_e,R_o}^2 = \frac{I_{\alpha_{R_e},R_o}}{m_{R_e,R_o} b^2}$$

$$\gamma_{\alpha R_e,R_o}^2 = \frac{\omega_{\alpha R_e,R_o}}{\omega_o}; \qquad \gamma = \frac{\omega_o^2}{\omega^2}$$

ω_o = reference frequency

The stability of the cascade is obtained by relating the frequency ratio γ to the exponent $(i\omega)$ as

$$i\omega/\omega_o = i/\sqrt{\gamma} = d \pm iv \tag{8}$$

Thus, a positive value for μ corresponds to an unstable cascade configuration.

The mathematical model specified by Eq. (5) represents both an aerodynamically and structurally detuned airfoil cascade and a tuned cascade in which all of the blades are structurally identical and uniformly spaced. Structural detuning is accomplished by varying the frequency ratios $\gamma_{\alpha_{R_e}}$ and $\gamma_{\alpha_{R_o}}$, coefficient $[CM^2]_{R_e,R_o}$ and $[CM^1]_{R_e,R_o}$.

Model Verification

The aeroelastic model developed herein utilizes a finite cascade analysis together with an influence coefficient technique to calculate the unsteady aerodynamic forces and moments. To verify the fundamentals of this model, it is first applied to Verdon's cascade B tuned airfoil cascade configuration, depicted in Fig. 4. Predictions from this model together

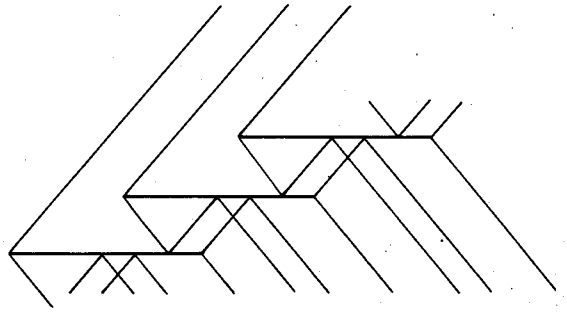

Fig. 4 Verdon's cascade B flow geometry.

with analogous predictions obtained from the model of Kielb and Kaza,[2] which utilizes the infinite cascade aerodynamic analysis of Adamczyk and Goldstein,[9] are present in Fig. 5. As seen, there is excellent agreement between the two models.

To verify the ability of this model to predict structural detuning effects, this model and that of Kielb and Kaza are both applied to the cascade B configuration with an alternate airfoil frequency detuning of 8%. For this structurally detuned cascade configuration, the phase plane results of these two independent predictions with the interblade phase angle as parameter are presented in Fig. 6. As seen, excellent agreement is again obtained.

Results

To demonstrate the effects of aerodynamic and structural detuning on supersonic unstalled flutter, the aeroelastic stability model specified by Eq. (7) is applied to a 12 bladed rotor, with Verdon's cascade B flow geometry as the baseline airfoil configuration.

Five separate configurations are considered. Case 1 is the baseline tuned rotor. Case 2 corresponds to alternate natural frequency detuning of 8% of the baseline rotor. Case 3 involves the aerodynamic detuning of the baseline rotor, accomplished by alternating the circumferential airfoil spacing by 13.3%. The remaining two cases correspond to combined structurally and aerodynamically detuned rotors. Case 4 has the set of odd-numbered airfoils at the higher frequency and the even-numbered airfoil set at the lower frequency, whereas Case 5 has the set of even-numbered airfoils at the higher frequency and the odd-numbered airfoil set at the lower frequency.

Figure 7 schematically depicts the flow geometry of the aerodynamically tuned and detuned rotors. As seen, the Mach wave/airfoil surface intersections are affected by the aerodynamic detuning, with different loading distributions on the sets of odd and even numbered airfoils. Hence, the need to consider cases 4 and 5.

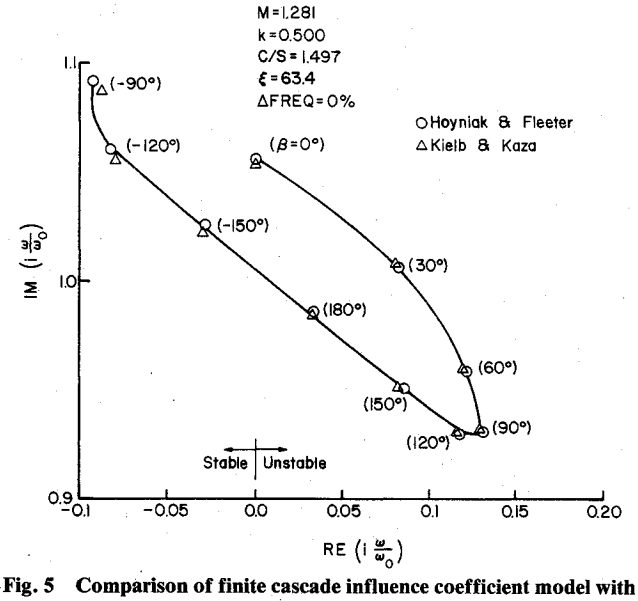

Fig. 5 Comparison of finite cascade influence coefficient model with infinite cascade conventional tuned cascade analysis.

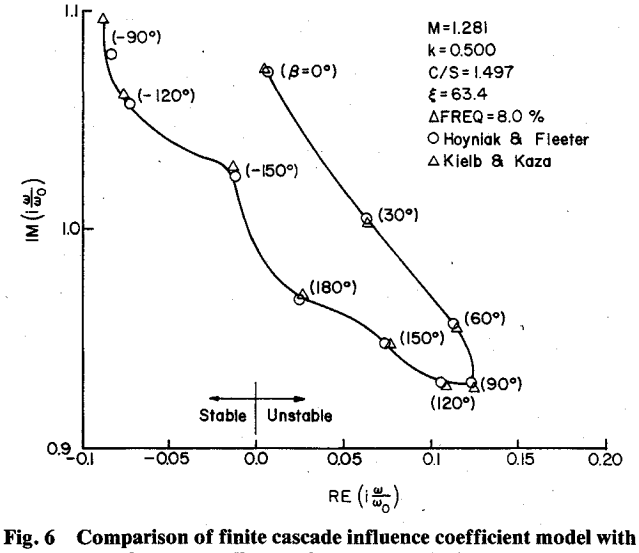

Fig. 6 Comparison of finite cascade influence coefficient model with infinite cascade structurally tuned cascade analysis.

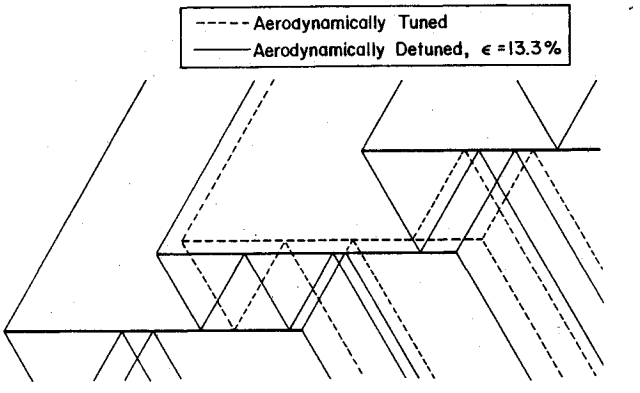

Fig. 7 Aerodynamically tuned and detuned cascade flow geometries.

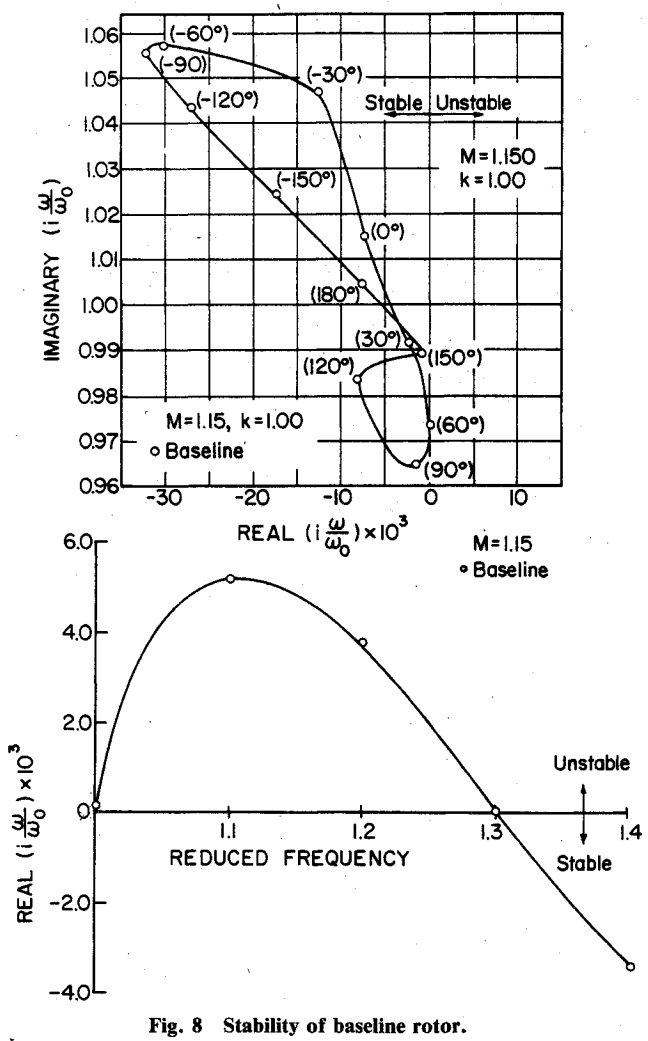

Fig. 8 Stability of baseline rotor.

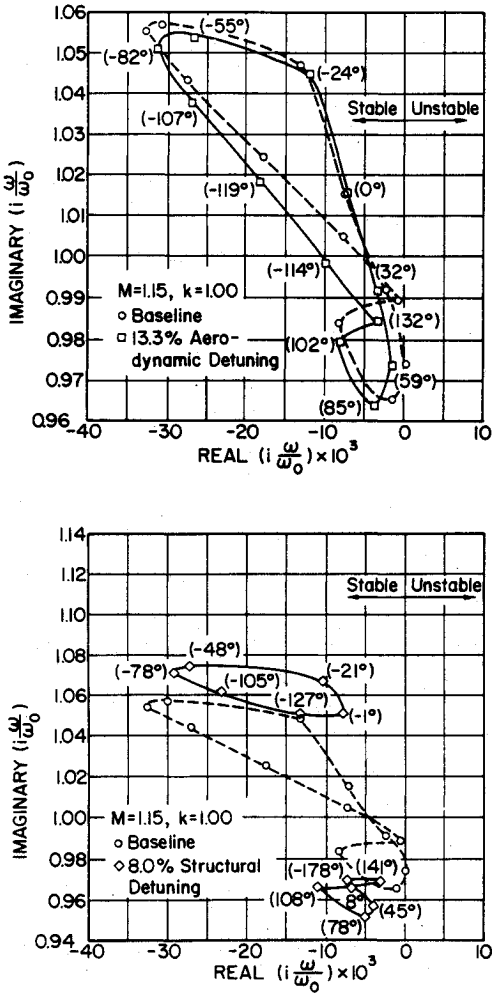

Fig. 9 Design point stability of structurally and aerodynamically detuned rotors.

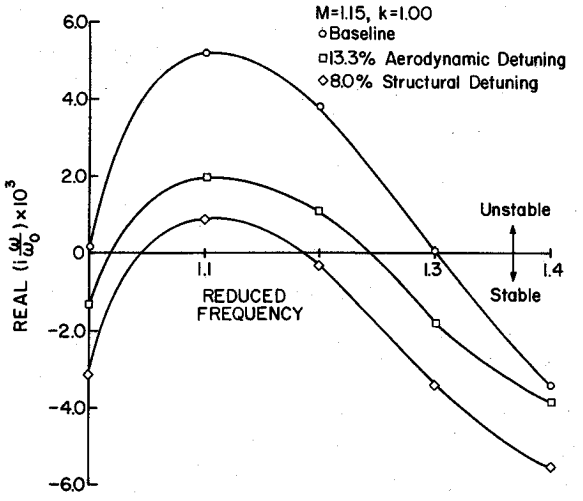

Fig. 10 Effect of reduced frequency on stability of aerodynamically and structural detuned rotors.

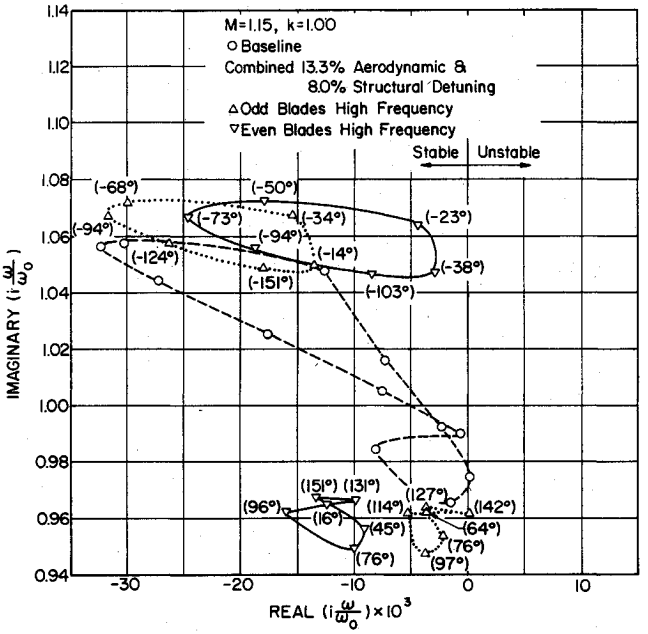

Fig. 11 Design point stability of combined aerodynamically and structurally detuned rotors.

The stability of the case 1 baseline tuned rotor at the nominal design point (Mach = 1.15, $k = 1.0$) with interblade phase angle as parameter and also as a function of reduced frequency at Mach = 1.15 is presented in Fig. 8. As seen in the lower portion of this figure, the baseline rotor is unstable for reduced frequency values between 1.0 and 1.3. At the design point, the baseline rotor is neutrally stable, with the least stable mode corresponding to a forward traveling wave characterized by an interblade phase angle of 60 deg.

The effect of the structural and the aerodynamic detuning, cases 2 and 3, on the stability of the baseline tuned rotor is demonstrated in Figs. 9 and 10. Both detuning mechanisms are seen to enhance stability, with the unstable reduced frequency range of the baseline rotor decreased by the aerodynamic and structural detuning: from ($1.0 < k < 1.3$) for the baseline, to ($1.02 < k < 1.25$) with aerodynamic detuning, and to ($1.06 < k < 1.18$) with structural detuning (Fig. 10).

Figures 11 and 12 show the effect of combined aerodynamic and structural detuning on stability (cases 4 and 5). At the design point, the combined detuning alters the least stable mode: a forward traveling wave with an interblade phase angle of 60 deg for the baseline case 1; 142 deg for the detuned rotor of case 4; a backward traveling wave with an interblade phase angle of −38 deg for the detuned rotor of case 5. However, the design point stability is enhanced only by the detuned rotor with the set of even-numbered airfoils at the higher frequency (case 5), the case 4 detuned rotor and the baseline rotor both being neutrally stable.

In terms of the reduced frequency (Fig. 12), combined aerodynamic and structural detuning enhances stability. With the set of odd-numbered airfoils at the higher frequency (case 4), the detuned rotor is unstable over the range $1.0 < k < 1.2$. However, with the set of even numbered airfoils at the higher frequency (case 5), the detuned rotor is stable for all reduced frequencies. Thus, the combination of aerodynamic and structural detuning is seen to significantly enhance the stability of the rotor, with the placement of the high- and low-frequency airfoils in the nonuniform circumferentially spaced rotor critical. This result is associated with the fundamental differences between the sets of even- and odd-numbered airfoils. In particular, as previously noted and depicted in Fig. 7, the sets of odd- and even-numbered airfoils have different Mach wave/airfoil surface intersection locations and unsteady aerodynamic loading distributions.

To demonstrate the fundamentals of the various detuning mechanisms, the design point chordwise distributions of the least stable mode unsteady perturbation pressure coefficient on the pressure and suction surfaces of the reference airfoils for the five cases considered are presented in Figs. 13-16.

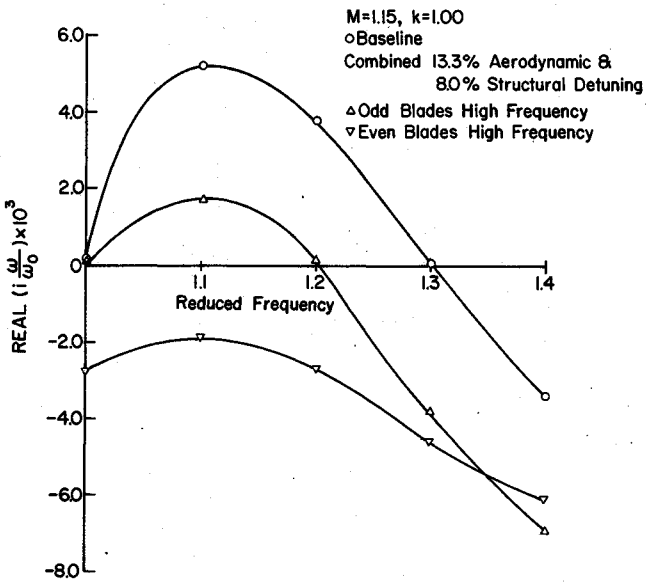

Fig. 12 Effect of reduced frequency on stability of combined aerodynamically and structurally detuned rotors.

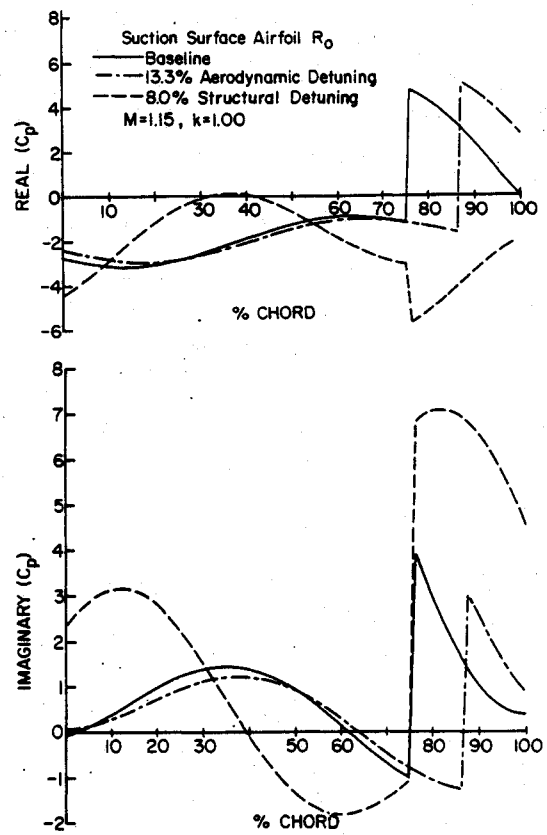

Fig. 13 Effect of aerodynamic and structural detuning on airfoil R_0 suction surface complex pressure distribution.

These can be interpreted as the nondimensional unsteady pressure distributions on the reference airfoils executing unit amplitude torsional motion. Thus, for the aerodynamically tuned cascade configurations, the integral of the moment of the difference across the chordline of these surface unsteady pressure coefficient distributions yields the standard moment coefficient as defined by Carta.[10]

Figures 13-16 present the real and imaginary parts of the unsteady perturbation pressure coefficients on the reference airfoils of the tuned, structurally detuned, and aerodynamically detuned rotor configurations (cases 1-3).

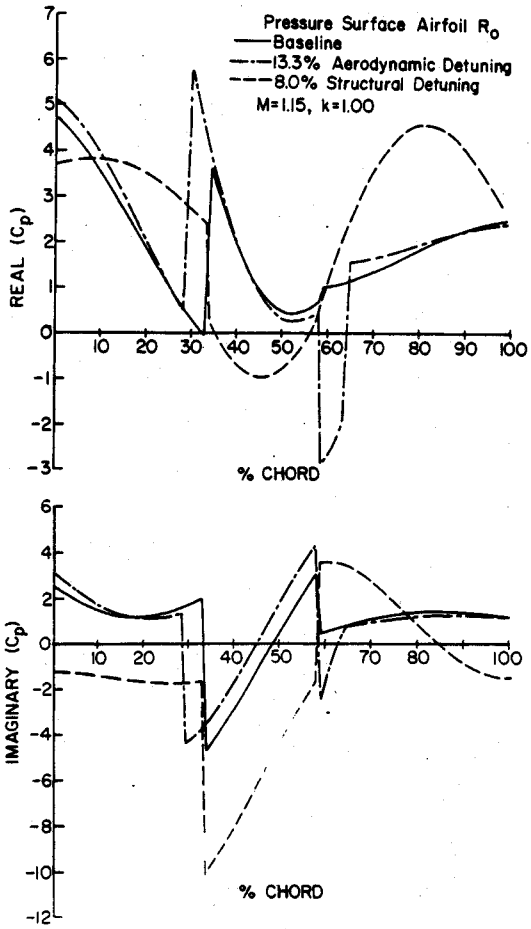

Fig. 14 Effect of aerodynamic and structural detuning on airfoil R_0 pressure surface complex pressure distribution.

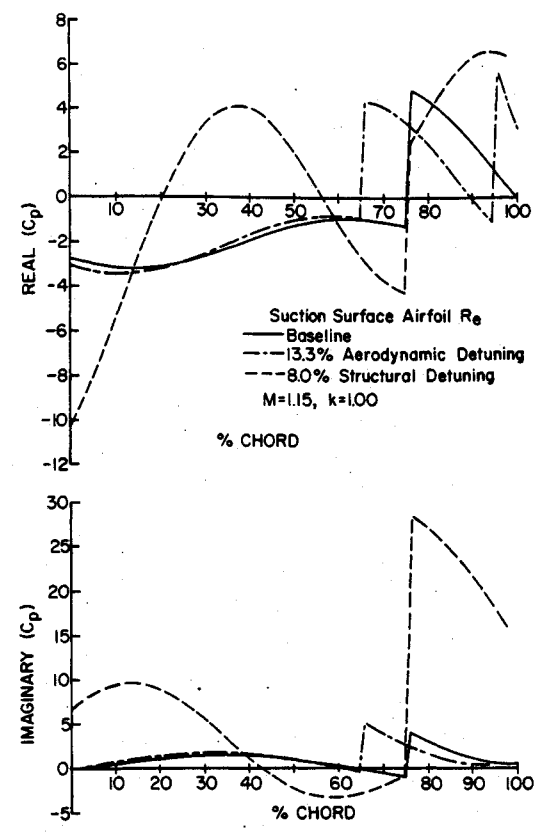

Fig. 15 Effect of aerodynamic and structural detuning on airfoil R_e suction surface complex pressure distribution.

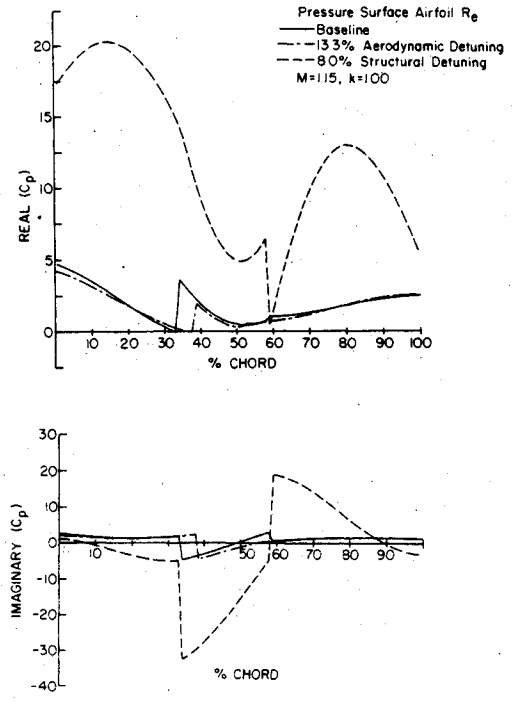

Fig. 16 Effect of aerodynamic and structural detuning on airfoil R_e pressure surface complex pressure distribution.

The primary effect that aerodynamic detuning has is on the location of the Mach wave/airfoil intersections, with the overall level of the unsteady perturbation pressure only slightly affected. Also, aerodynamic detuning has only a small effect on the flutter mode. Thus, the enhanced stability associated with the aerodynamic detuning of case 3 is a result of the changes in the Mach/wave airfoil intersections apparent in Fig. 10.

Structural detuning (case 2) has a large effect on the flutter mode and also on the overall level of the unsteady airfoil loading. This latter effect is due to the change in the least stable mode, characterized by the interblade phase angle, associated with this structural detuning. Hence, the increased stability enhancement of structural detuning as compared to aerodynamic detuning, as seen in Figs. 9 and 10.

Summary and Conclusions

An aeroelastic model has been developed to investigate the enhanced supersonic unstalled flutter stability of a turbomachine rotor associated with both structural and aerodynamic detuning. In this model, alternate blade structural detuning is considered. The aerodynamic detuning is accomplished by means of nonuniform circumferential spacing of adjacent rotor blades. The unsteady aerodynamic forces and moments are developed in terms of influence coefficients in a manner that enables the stability of both a conventional aerodynamically tuned rotor as well as the detuned rotor configurations to be determined.

This aeroelastic model was used to demonstrate the effects of combined aerodynamic and structural detuning on the aeroelastic stability of a 12 bladed rotor, with Verdon's cascade B flow geometry as a baseline configuration. Aerodynamic and structural detuning were shown to enhance stability, although neither technique when applied separately stabilized the rotor over the the complete reduced frequency range considered. The aerodynamic detuning directly affected the unsteady airfoil loading whereas structural detuning altered the flutter mode and, subsequently, the unsteady loading.

The greatest stability enhancement, with the resulting rotor stable over the complete range of reduced frequencies, resulted from a combination of aerodynamic and structural detuning. The placement of the high- and low-frequency airfoils in the nonuniformly spaced rotor was significant with regard to stability, affecting both the unsteady aerodynamic loading and the flutter mode. Thus, combined aerodynamic and structural detuning appears to be a viable passive flutter control mechanism for the stability enhancement of a rotor with regard to supersonic unstalled flutter.

Acknowledgment

The NASA Lewis Research Center and, in particular, Don Boldman and Calvin Ball, are most gratefully acknowledged for their encouragement, discussions, and support.

References

[1]Whitehead, D.S., "Effect of Mistuning on the Vibration of Turbomachine Blades Induced by Wakes," *Journal of Mechanical Engineering Science,* Vol. 8, No. 1, March 1966, pp. 15-21.

[2]Kaza, K.R.V. and Kielb, R.E., "Effect of Mistuning on Bending-Torsion Flutter and Response of a Cascade in Incompressible Flow," *AIAA Journal,* Vol. 20, Aug. 1982, pp. 1120-1127.

[3]Kielb, R.W. and Kaza, K.R.V., "Aeroelastic Characteristics of Mistuned Blades in Subsonic and Supersonic Flows," *Journal of Vibration, Stress, and Reliability in Design,* Vol. 105, Oct. 1983, pp. 425-433.

[4]Bendiksen, O.O., "Flutter of Mistund Turbomachinery Rotors," ASME Paper 83-GT-153, 1983.

[5]Crawley, E.F. and Hall, K.C., "Optimization and Mechanisms of Mistuning of Cascades," ASME Paper 84-GT-196, 1984.

[6]Verdon, J.M. and McCune, J.E., "The Unsteady Supersonic Cascade in Subsonic Axial Flow," *AIAA Journal,* Vol. 13, Feb. 1975, pp. 193-201,

[7]Brix, C.W. and Platzer, M.F., "Theoretical Investigation of Supersonic Flow Past Oscillating Cascades with Subsonic Leading Edge Locus," AIAA Paper 74-14, Jan. 1974.

[8]Caruthers, J.E. and Riffel, R.E., "Aerodynamic Analysis of a Supersonic Cascade Vibrating in a Complex Mode," *Journal of Sound and Vibration,* Vol. 71, 1980, pp. 425-433.

[9]Adamczyk, J.J. and Goldstein, M.E., "Unsteady Flow in a Supersonic Leading Edge Locus," *AIAA Journal,* Vol. 16, Dec. 1979, pp. 1248-1254, pp. 425-433.

[10]Carta, F.O., "Aeroelasticity and Unsteady Aerodynamics," *Aerothermodynamics of Gas Turbine Engines,* AFAPL TR 78-52, 1978, pp. 22-1, 22-54.